

Numerical investigation of cold spray gas particle dynamics

S. Li¹, J. Soria¹, B. Muddle² & M. Jahedi³

¹Laboratory for Turbulence Research in Aerospace & Combustion, Department of Mechanical Engineering, Monash University,

²ARC Centre of Excellence for Design in Light Metals, ³CSIRO, Manufacturing and Materials Technology
email: Shuo.Li@eng.monash.edu.au

Introduction

• Cold-gas dynamic spray process (Figure 1) is a coating technique in which solid particles are deposited onto a substrate at supersonic speeds

• Detrimental effects associated with liquefaction such as temperature oxidation, evaporation, melting, residual stresses are minimised

• The flow field between the nozzle exit and the substrate is that of a two phase gas particle supersonic impinging jet

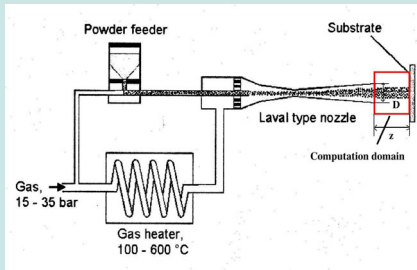


Figure 1: Coldspray process. [1]

• Figure 2 is a flow visualisation of a supersonic impinging gas jet obtained using shadowgraphy

• It reveals the main flow features including a standoff shock, jet shock and jet boundary

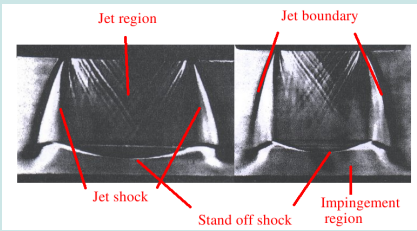


Figure 2: Supersonic impinging jet at $PR = 3$, (Left) $s = 2$ (Right) $s = 3$. [2]

Aim

• Aim of the project is to investigate the gas particle interaction for both planar and round supersonic impinging jets

• This poster presents results for supersonic impinging gas jets issued from planar and round nozzles

• The flow is parameterised by the nozzle exit pressure ratio PR , Mach number Ma and impingement distance s (standoff distance)

$$PR = \frac{P'_e}{P'_{ambient}}, \quad Ma = \frac{u'_e}{c'_e}, \quad s = \frac{z}{D}$$

Numerical method

• The two-dimensional cartesian ($\alpha = 0$) and cylindrical ($\alpha = 1$) Euler equations (Equation 1) are used to simulate the planar and radial jet respectively

$$\frac{\partial \mathbf{U}}{\partial t} + \frac{\partial \mathbf{F}}{\partial x} + \frac{\partial \mathbf{G}}{\partial r} + \alpha \mathbf{S} = 0 \quad (1)$$

$$\mathbf{U} = \begin{bmatrix} \rho \\ \rho u \\ e \end{bmatrix}, \quad \mathbf{F} = \begin{bmatrix} \rho u \\ (\rho u^2 + P) \\ (e + P)u \end{bmatrix}, \quad \mathbf{S} = \begin{bmatrix} \rho u \\ \rho u^2 \\ (e + P)u \end{bmatrix}$$

• The internal energy per unit volume e assuming an ideal gas is given by Equation 2

$$e = \frac{P}{\gamma - 1} + 0.5\rho u^2 \quad (2)$$

• The dimensionless variables ρ, P, u, v and t are:

$$P = \frac{P'}{P'_e}, \quad \rho = \frac{\rho'}{\rho'_e}, \quad t = \frac{t'c'_e}{D},$$

$$(u, v) = \frac{(u', v')}{c'_e}, \quad (x, r) = \frac{(x', r')}{D}$$

• Subscript 'e' refers to properties at the nozzle exit while the ' ' refer to dimensional variables

• The governing equations are solved using a symmetric total variation diminishing (TVD) scheme [5] with the appropriate boundary conditions from [4]

Simulation results

• Figures 3 and 4 are the dimensionless velocity magnitude and pressure contours of a planar supersonic impinging jet

• Figures 6 and 7 are the dimensionless velocity magnitude and pressure contours of a round supersonic impinging jet

• Figure 5 and 8 are 'numerical shadowgraphs' calculated from Equation 3

$$\frac{\partial^2 \rho'}{\partial x'^2} + \frac{\partial^2 \rho'}{\partial y'^2} \quad (3)$$

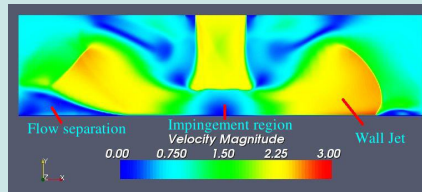


Figure 3: Planar supersonic impinging jet at $PR = 1.2, Ma = 2.2, s = 2$.

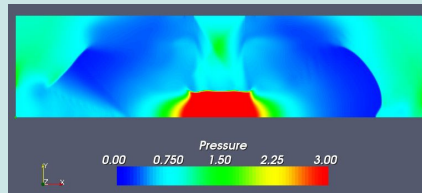


Figure 4: Planar supersonic impinging jet at $PR = 1.2, Ma = 2.2, s = 2$.

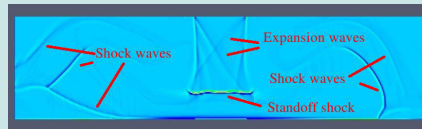


Figure 5: Planar supersonic impinging jet at $PR = 1.2, Ma = 2.2, s = 2$.

• The planar supersonic impinging jet is asymmetrical with wall jets the size of the exit jet

• The round supersonic impinging jet has a much smaller wall jet along the plate

• Figure 9 is the pressure distribution along the substrate

• The maximum pressure of the planar impinging jet is considerably greater than the round impinging jet

• For the round impinging jet the pressure near the jet centerline is lower than that of experiment data [3]

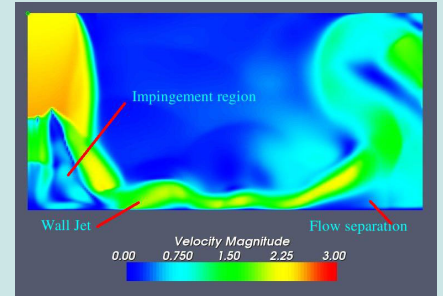


Figure 6: Round supersonic impinging jet at $PR = 1.2, Ma = 2.2, s = 2$.

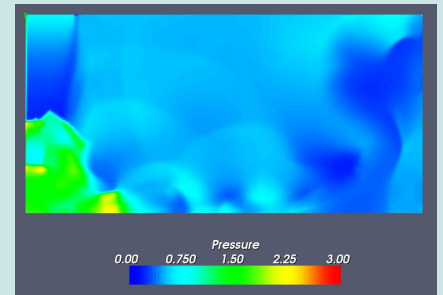


Figure 7: Round supersonic impinging jet at $PR = 1.2, Ma = 2.2, s = 2$.



Figure 8: Round supersonic impinging jet at $PR = 1.2, Ma = 2.2, s = 2$.

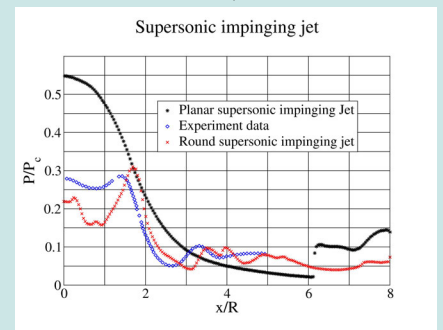


Figure 9: Supersonic impinging jet at $PR = 1.2, Ma = 2.2, s = 2$.

• The outflow boundary condition appears to induce flow separation of the wall jet

References

- [1] Edited by J.R. Davis. *Handbook of thermal spray technology*. Copublished by the Thermal Spray Society and ASM International, 1st edition, 2004.
- [2] J.H. Gummer and B.L. Hunt. The impingement of non-uniform, axisymmetric supersonic jets on a perpendicular flat plate. *Israel Journal of Technology*, 12:221-235, 1974.
- [3] P.J. Lamont and B.L. Hunt. The impingement of underexpanded, axisymmetric jets on perpendicular and inclined flat plates. *J. Fluid Mech.*, 100(3):471-511, 1980.
- [4] U. Lei and Sy-Wen Liu. Some inviscid features of the normal impingement of an axisymmetric supersonic jet on a flat plate. *Journal of the Chinese Society of Mechanical Engineers*, 15(4):3370-351, 1994.
- [5] H.C. Yee. High resolution shock-capturing schemes for inviscid and viscous hypersonic flows. *Journal of Computational Physics*, 88:31-61, 1990.